MAG-GIC: Geomagnetically Induced Currents risk hazard in the Portuguese power network

Joana Alves Ribeiro[1,2,3], Maria Alexandra Pais[1,2], Fernando J. G. Pinheiro[1,2], Fernando A. Monteiro Santos[3]

[1] University of Coimbra, CITEUC, Department of Physics, Coimbra, Portugal
[2] University of Coimbra, CITEUC, Geophysical and Astronomical Observatory, Coimbra, Portugal
[3] University of Lisbon, Instituto Dom Luiz, Faculty of Sciences, Lisbon, Portugal

EGU 2020: Sharing Geoscience Online

Motivation

What are the major impacts of Space weather?

- Space-based telecommunications
- Broadcasting
- Weather services
- Navigation
- Power distribution
- Terrestrial communications

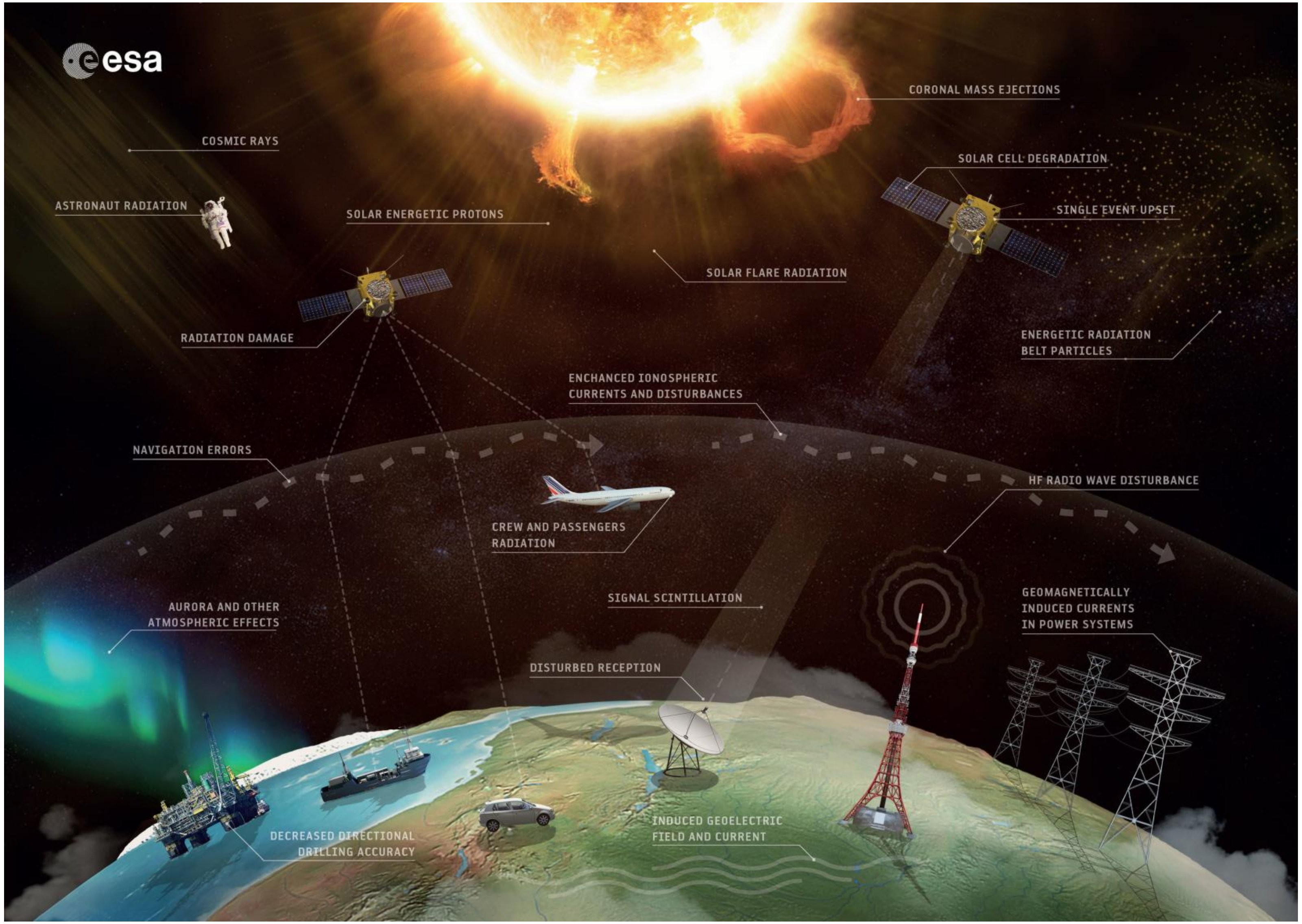

Credit: European Space Agency

Motivation

Ionospheric currents

Spatiotemporal variations produce variations in the Earth's geomagnetic field

Faraday's law of induction

Electric field induced at the Earth's surface and below

Geomagnetic Induced Currents GIC's

Flow in any conducting structure

e.g.: a power or pipeline grid grounded in the Earth

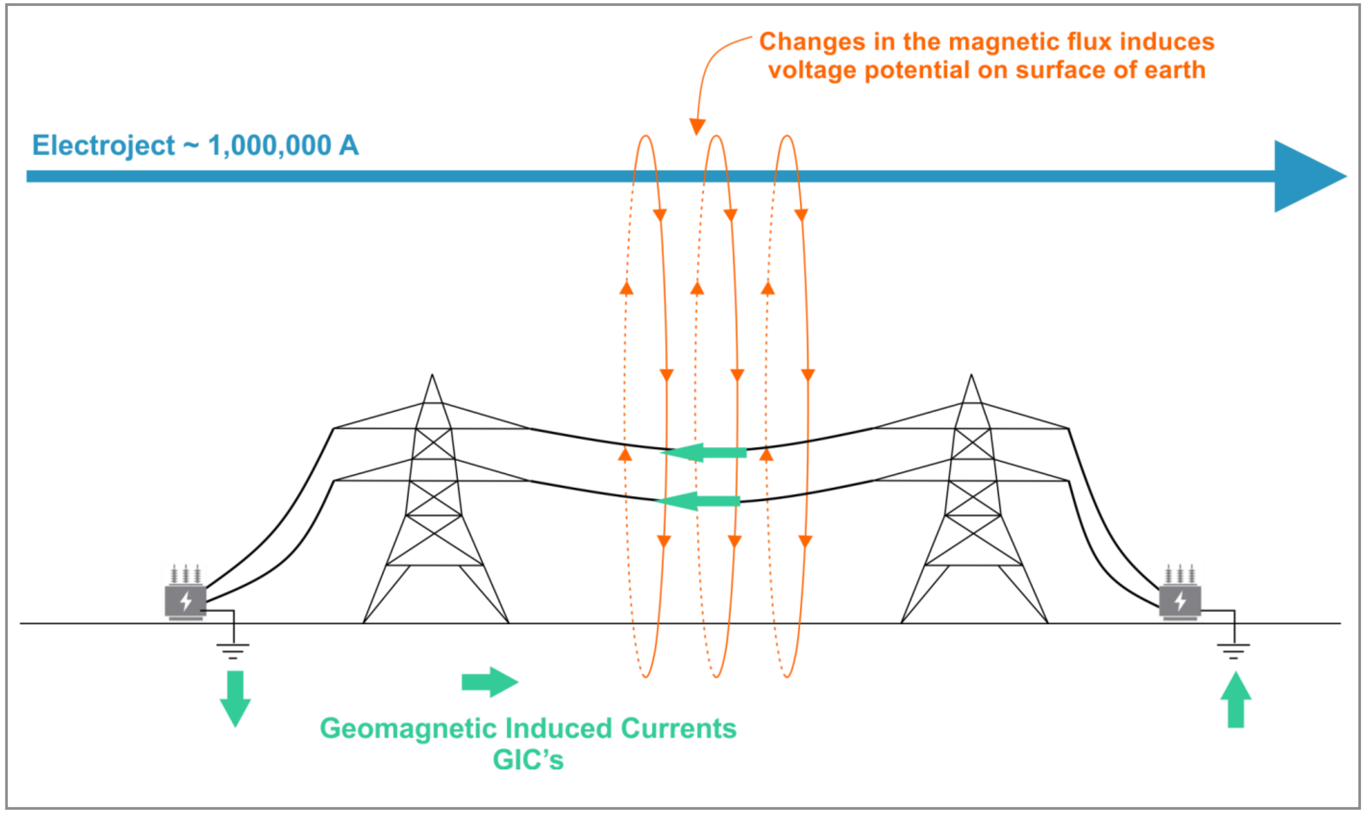

Motivation

Consequences of GIC's in the power network?

(Molinski, 2002)

- Transformer half-cycle saturation
- Transformer var consumption—system voltage Collapse
- Harmonics
- Transformer heating
- Generator heating
- Protective relaying problems
- Communication problems

Example of a transformer coil that overheated.

Governing Equations

- **Nodal Admittance Matrix method**
- **LP Method** (Lehtinen & Pirjola, 1985)

Mathematically equivalent
(Boteler & Pirjola, 2014)

$$\boldsymbol{I}^e = (\mathbb{1} + \boldsymbol{Y}^n \boldsymbol{Z}^e)^{-1} \boldsymbol{J}^e$$

Governing Equations

$$\boxed{I^e} = (\mathbb{1} + \underbrace{Y^n}_{\text{Network Admittance matrix}} \underbrace{Z^e}_{\text{Earthing impedance matrix}})^{-1} \underbrace{J^e}_{\text{Perfect earthing currents}}$$

GICs through earthing resistance

Numerical implementation based on GEOMAGICA (Bailey et al., 2017)

Governing Equations

$$\boxed{I^e} = (\mathbb{1} + Y^n Z^e)^{-1} J^e$$

GICs

Power Network

$$Z^e_{ij} = \delta_{ij} \boxed{R^e_j}$$

$$Y^n_{ij} = \begin{cases} -\dfrac{1}{\boxed{R^n_{ij}}}, & i \neq j \\ \displaystyle\sum_{k \neq i} \dfrac{1}{\boxed{R^n_{ij}}}, & i = j \end{cases}$$

Geomagnetic Storms

$$J^e_i = -\sum_{j \neq i} \frac{\boxed{V^o_{ij}}}{R^n_{ij}}$$

R^e_j – Resistance through the node i is earthed; R_{ij} – Resistance between nodes i and j; V^0_{ij} – Voltage from nodes i to j.

Area of Study

South of Portugal

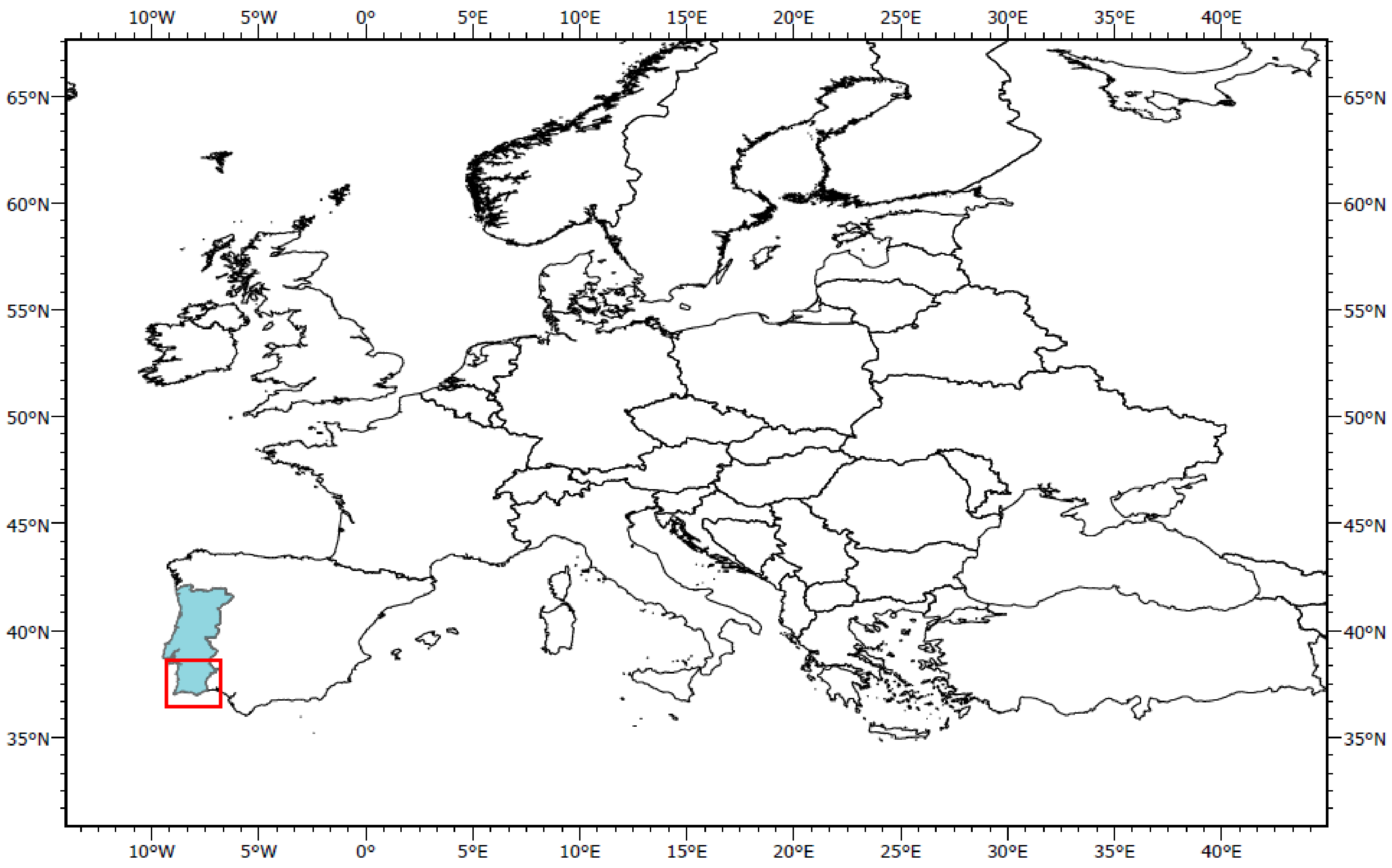

Area of Study

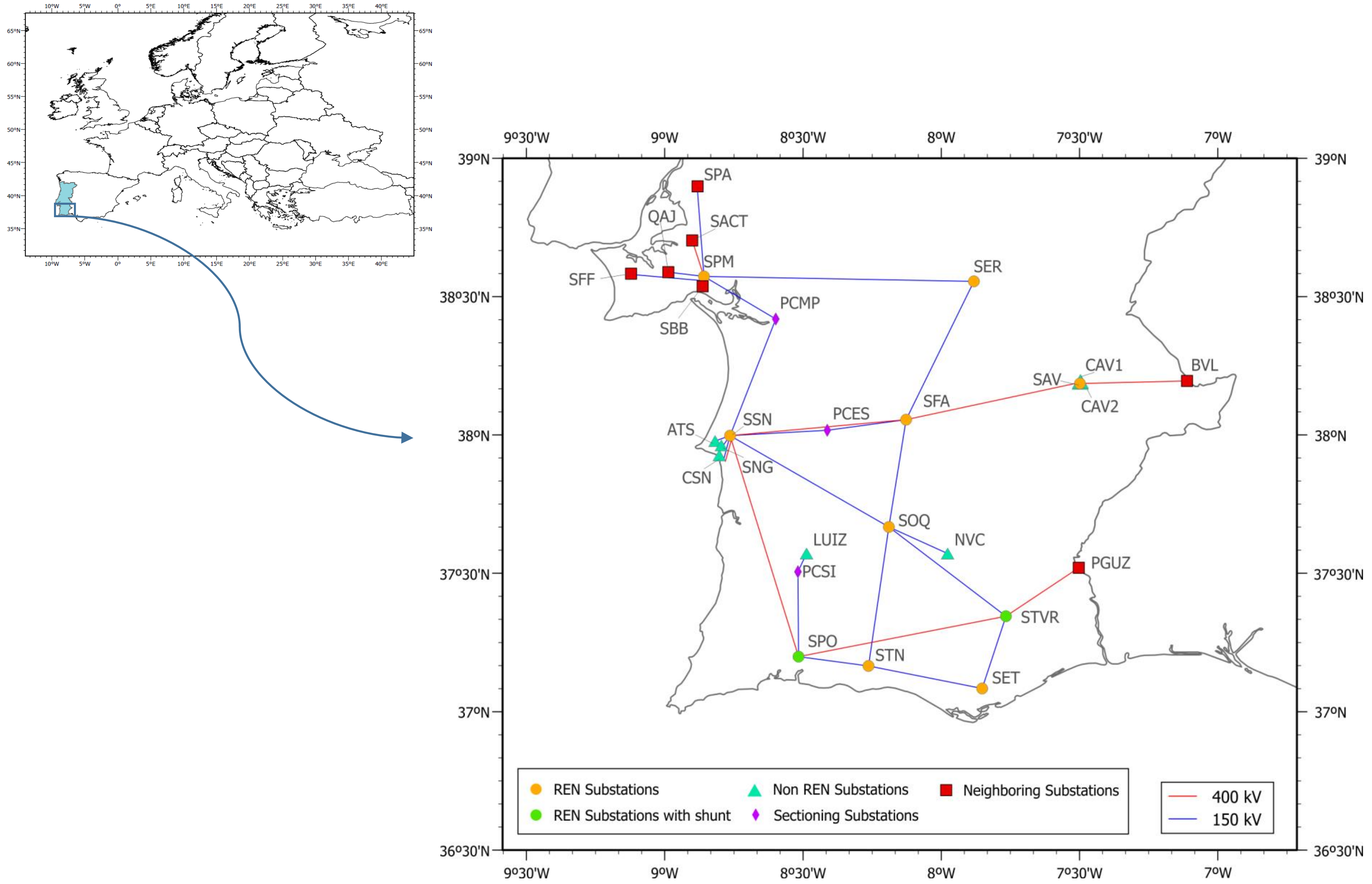

Full collaboration

- Location of substations and their ground resistance;
- Characterization of each transformer (type, winding resistance for high and low voltage);
- Transmission line information (length and line resistance).

Area of study

One-line Diagram

20 Substations

1 to 5 transformers

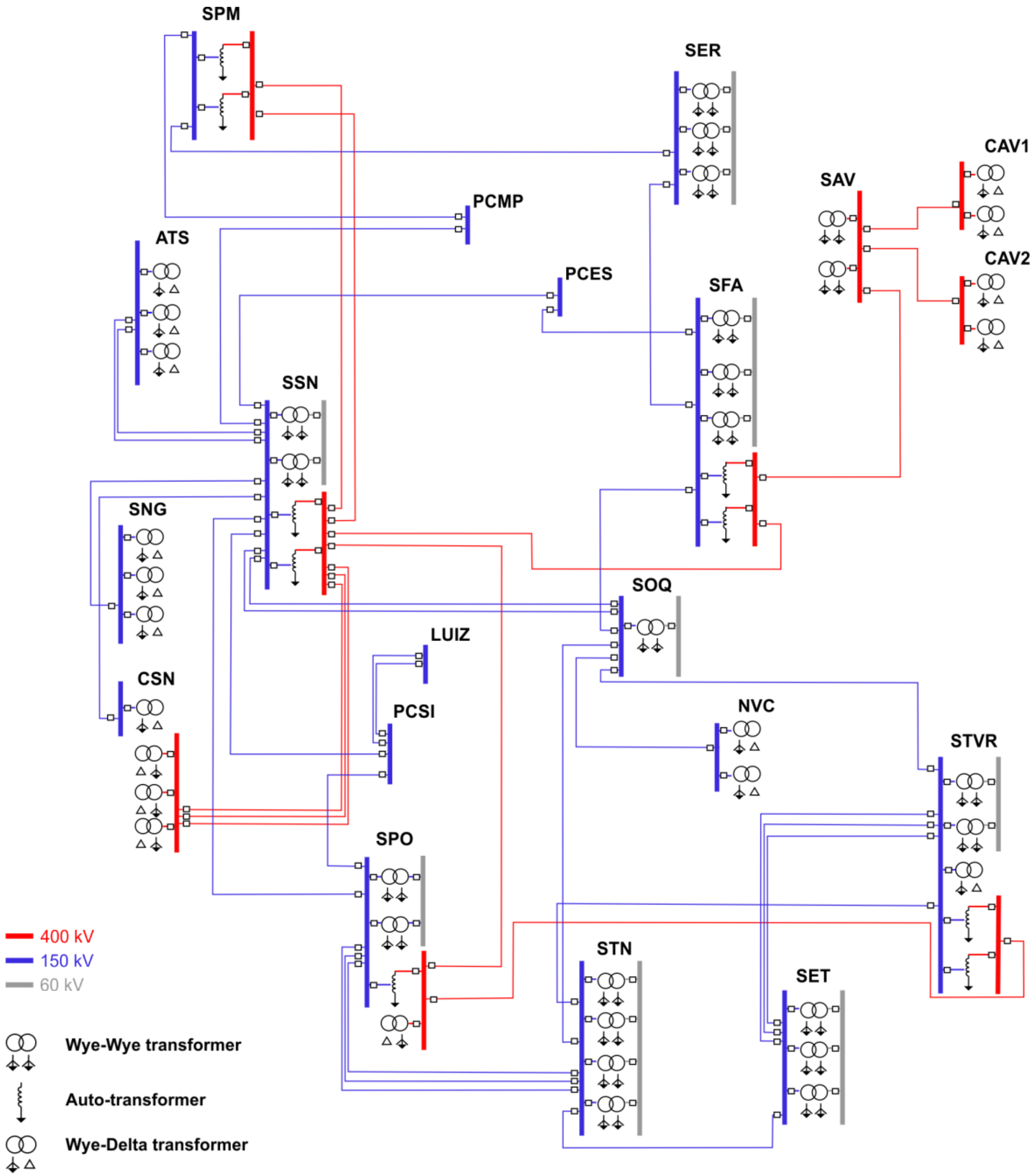

REN Substations

SPM - Palmela
SER - Évora
SAV - Alqueva
SFA - Ferreira do Alentejo
SSN - Sines
SOQ - Ourique
STRV - Tavira
SPO - Portimão
STN - Tunes
SET - Estói

Non REN Substations

CAV1 - Central Alqueva 1
CAV2 - Central Alqueva2
ATS - Artland (Sines)
NVC - Neves Corvo (SOMINCOR)
SNG - Sines Cogeração (GALP)
CSN - Central de Sines
LUIZ - Luizianes

Sectioning Subtations

PCMP - Monte da Pedra
PCES - Ermida do Sado
PCSI - Sabóia

Area of study

Equivalent circuit for Neighboring Networks

Northern Portuguese network

- SPM connected to 5 substations

Spanish network - REE

- STVR connected to 1 substation
- SAV connected to 1 substation

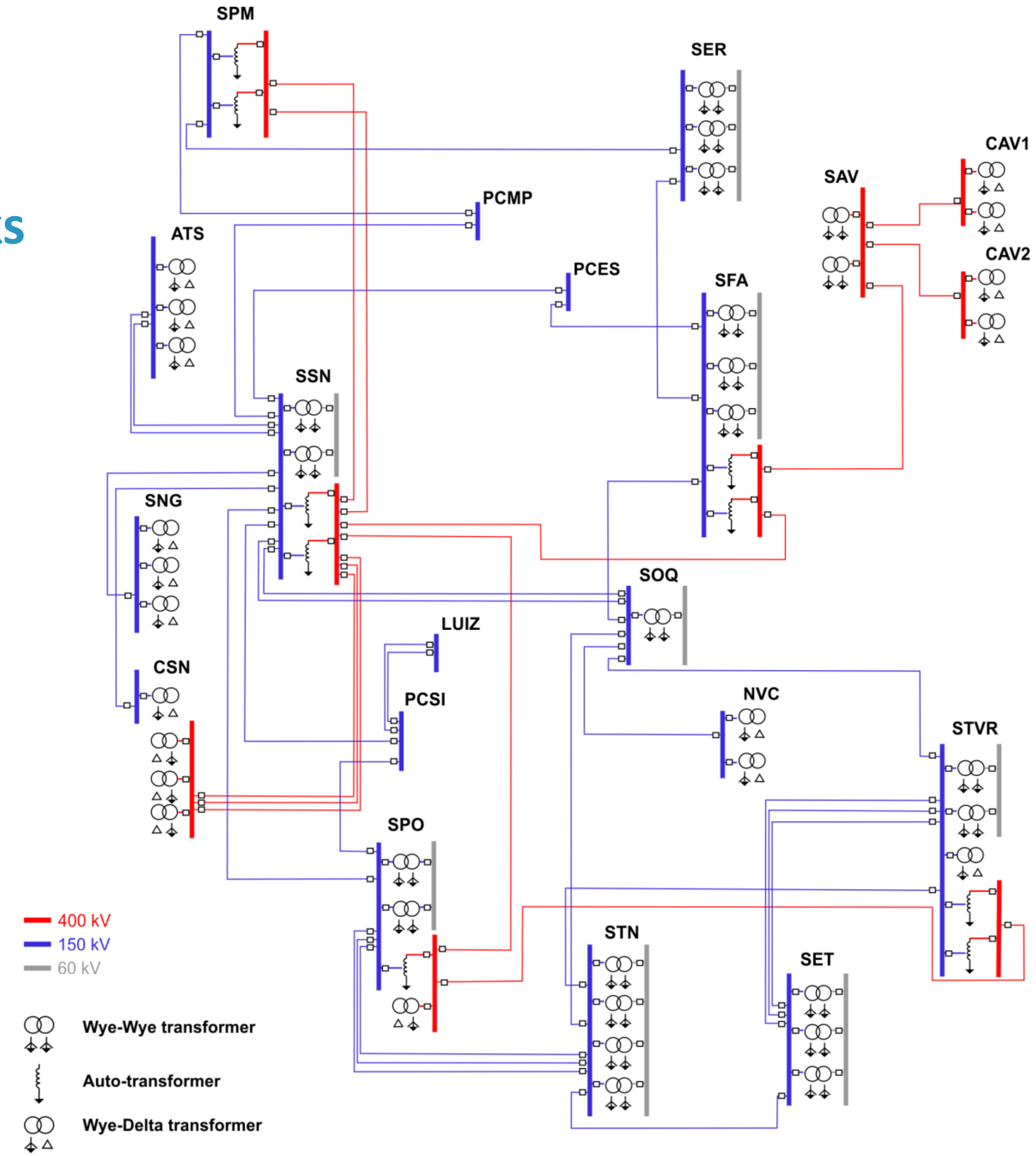

REN Substations

SPM - Palmela
SER - Évora
SAV - Alqueva
SFA - Ferreira do Alentejo
SSN - Sines
SOQ - Ourique
STRV - Tavira
SPO - Portimão
STN - Tunes
SET - Estói

Non REN Substations

CAV1 - Central Alqueva 1
CAV2 - Central Alqueva2
ATS - Artland (Sines)
NVC - Neves Corvo (SOMINCOR)
SNG - Sines Cogeração (GALP)
CSN - Central de Sines
LUIZ - Luizianes

Sectioning Subtations

PCMP - Monte da Pedra
PCES - Ermida do Sado
PCSI - Sabóia

Area of study

Equivalent circuit for Neighboring Networks

Northern Portuguese network

- SPM connected to 5 substations

Spanish network - REE

- STVR connected to 1 substation
- SAV connected to 1 substation

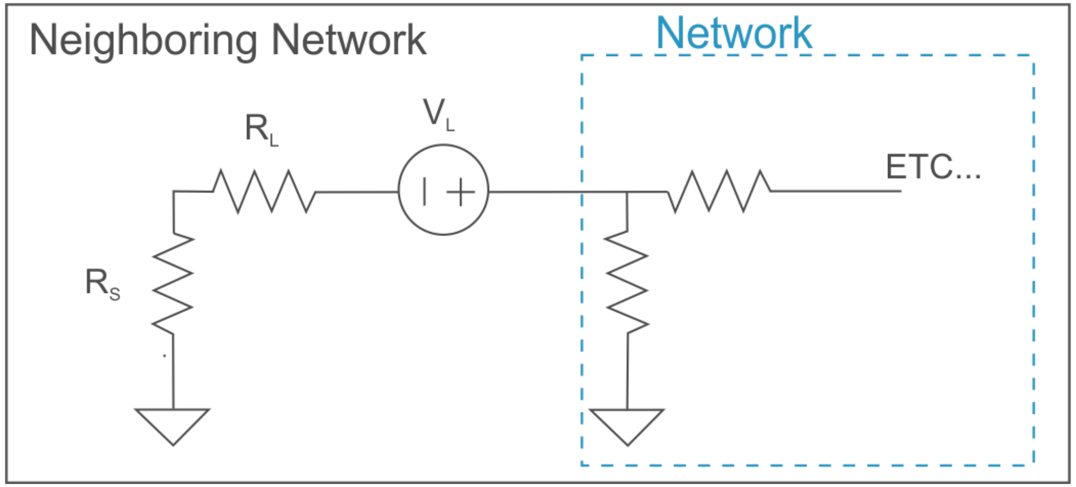

Equivalent Circuit 2 (EQC-2) from *Boteler et al, 2013*.
R_S – substation grounding resistance; R_L – Line resistance; V_L – Line voltage.

Thevenin equivalent circuit

$$\begin{cases} V_{th} = V_L \\ R_{th} = R_S + R_L \end{cases}$$

Uniform Electric Field (1 V/km)

Electric field of 1 V/km → **Extreme geomagnetic storm**

↓

Allows to evaluate the:

- Vulnerability of substations;
- Vulnerability of different sections of the network.

Uniform Electric Field (1 V/km)

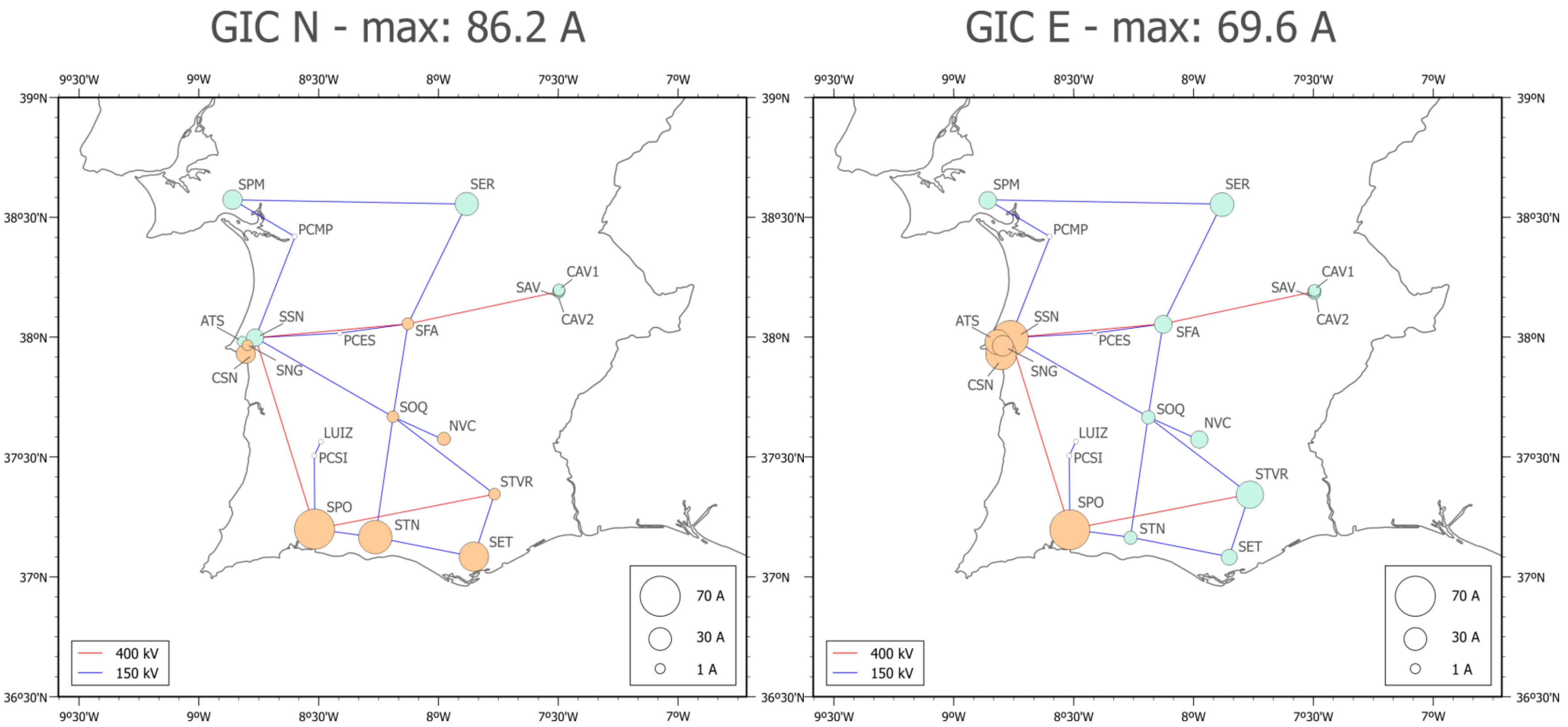

GIC at each substation in the Beta area under a northward (left) and eastward (right) electric field (geen into, orange out of the ground.

What influences GICs?

- Line length
- Line voltage
- Line Orientation
- Number of connections between substations
- Transformers characteristics
- “Edge Effect”

Uniform Electric Field (1 V/km)

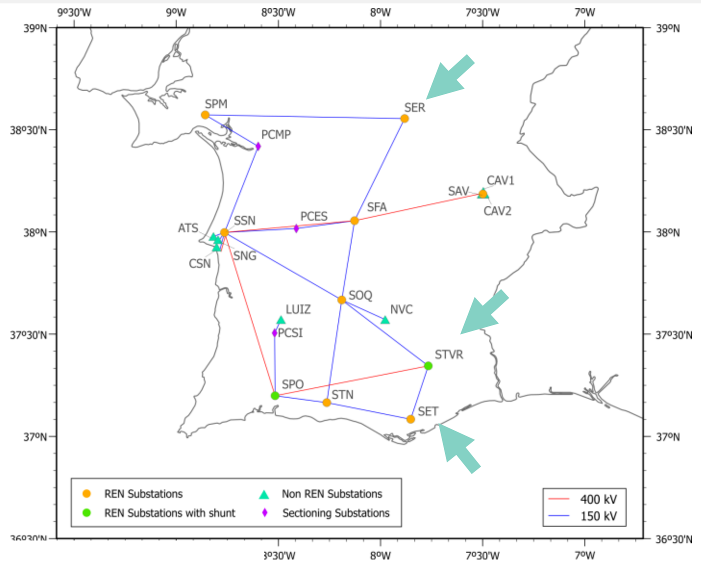

Directional Sensitivity

(Boteler & Pirjola, 2017)

$$GIC = GIC_N cos\theta + GIC_E sin\theta$$

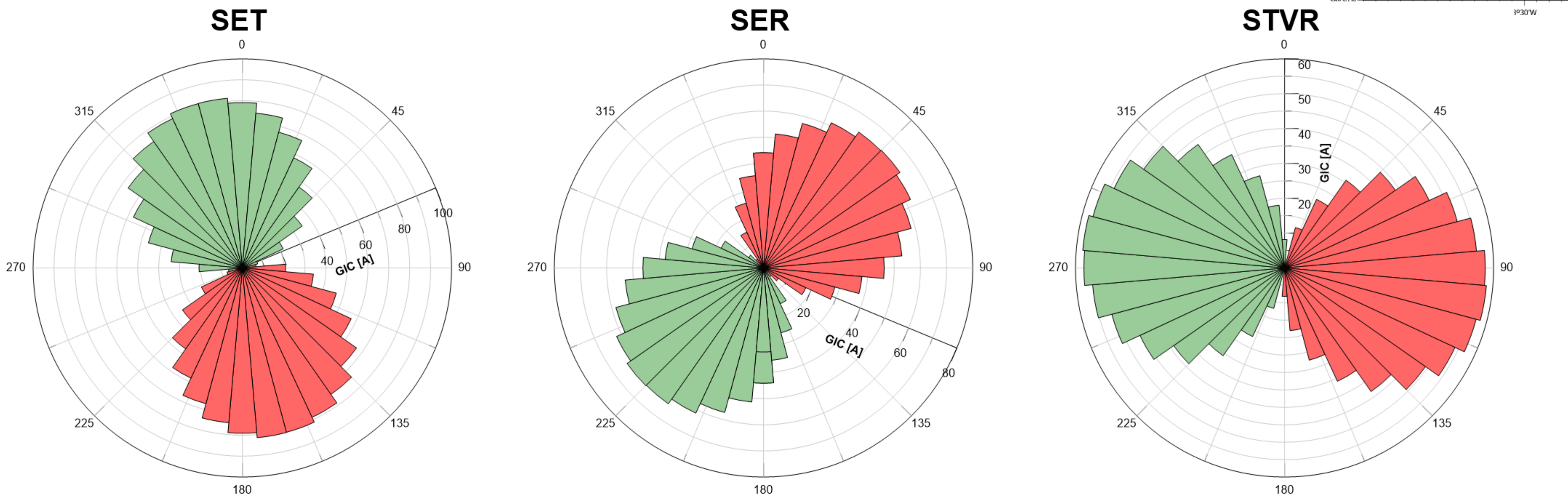

Directional sensitivity for SET, SER and STRV substations.

Uniform Electric Field (1 V/km)

Directional Sensitivity

(Boteler & Pirjola, 2017)

$$\theta_{peak} = \arctan\frac{GIC_E}{GIC_N}$$

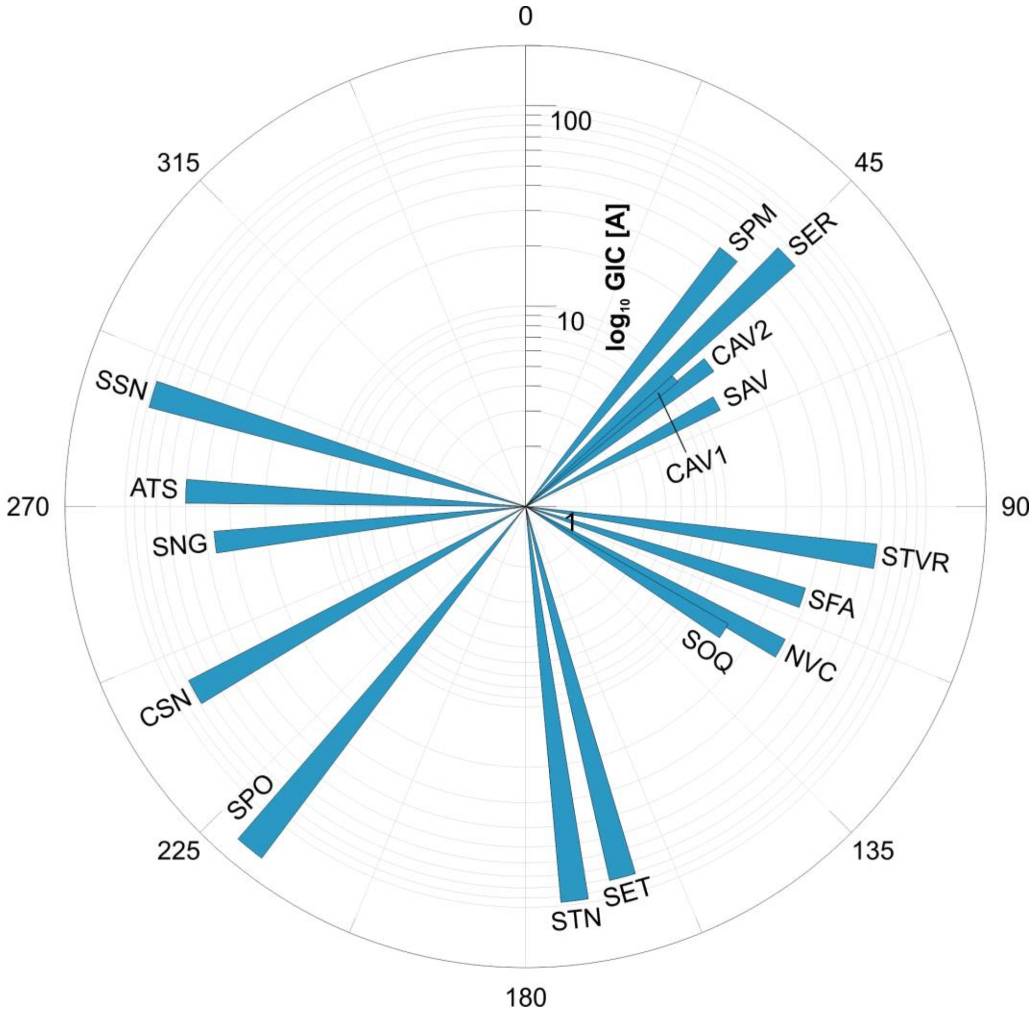

Orientation of the uniform electric field that produces the peak GIC value for each substation. The length of the bars represents the maximum GIC value.

Uniform Electric Field (1 V/km)

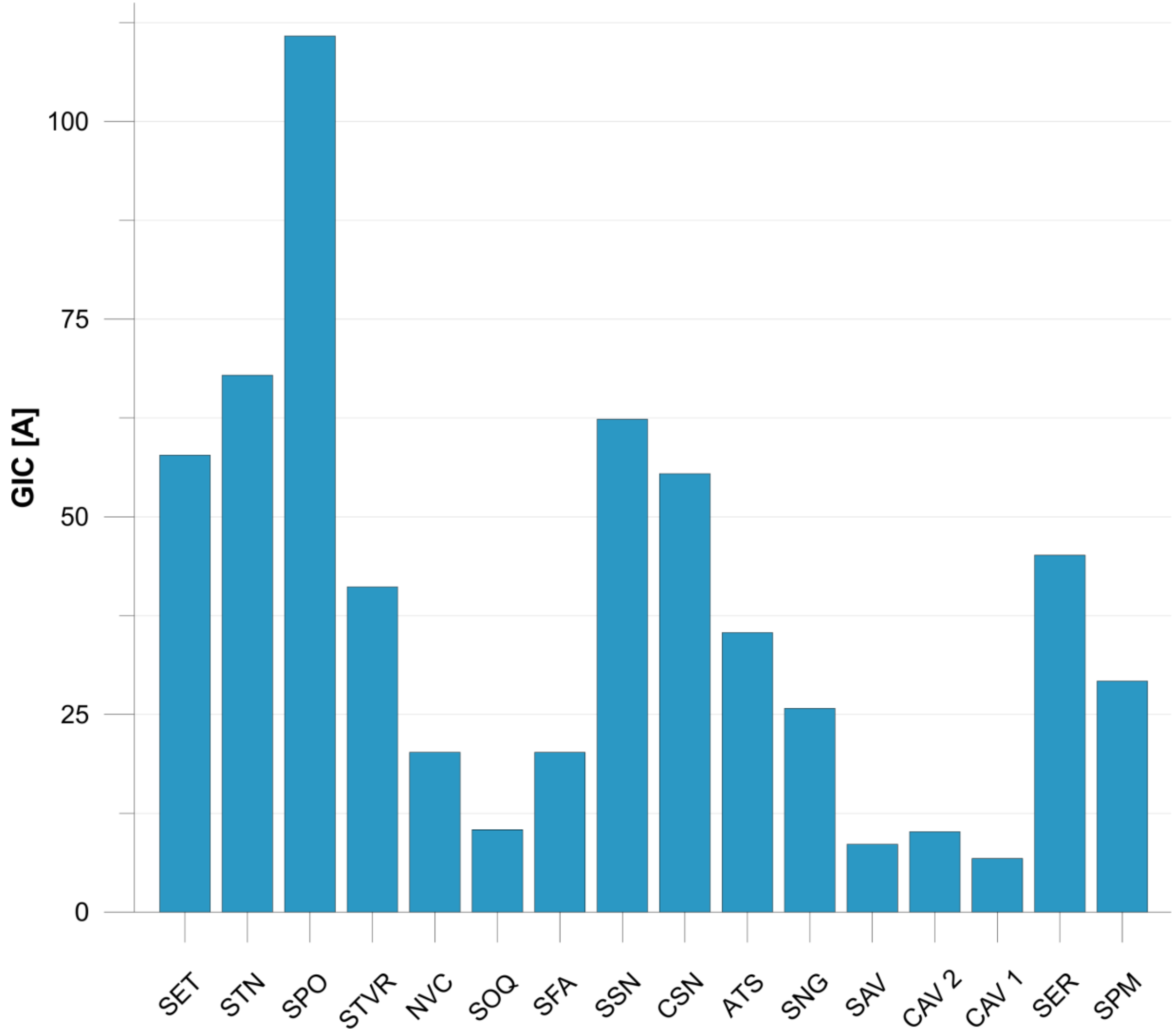

GIC_{peak} results in each substation for a uniform electric field.

$$GIC_{peak} = \sqrt{GIC_N^2 + GIC_E^2}$$

Most vulnerable

SPO substation

Uniform Electric Field (1 V/km)

GIC per transformer

Most vulnerable

Autotransformers in general, in particular for SPO

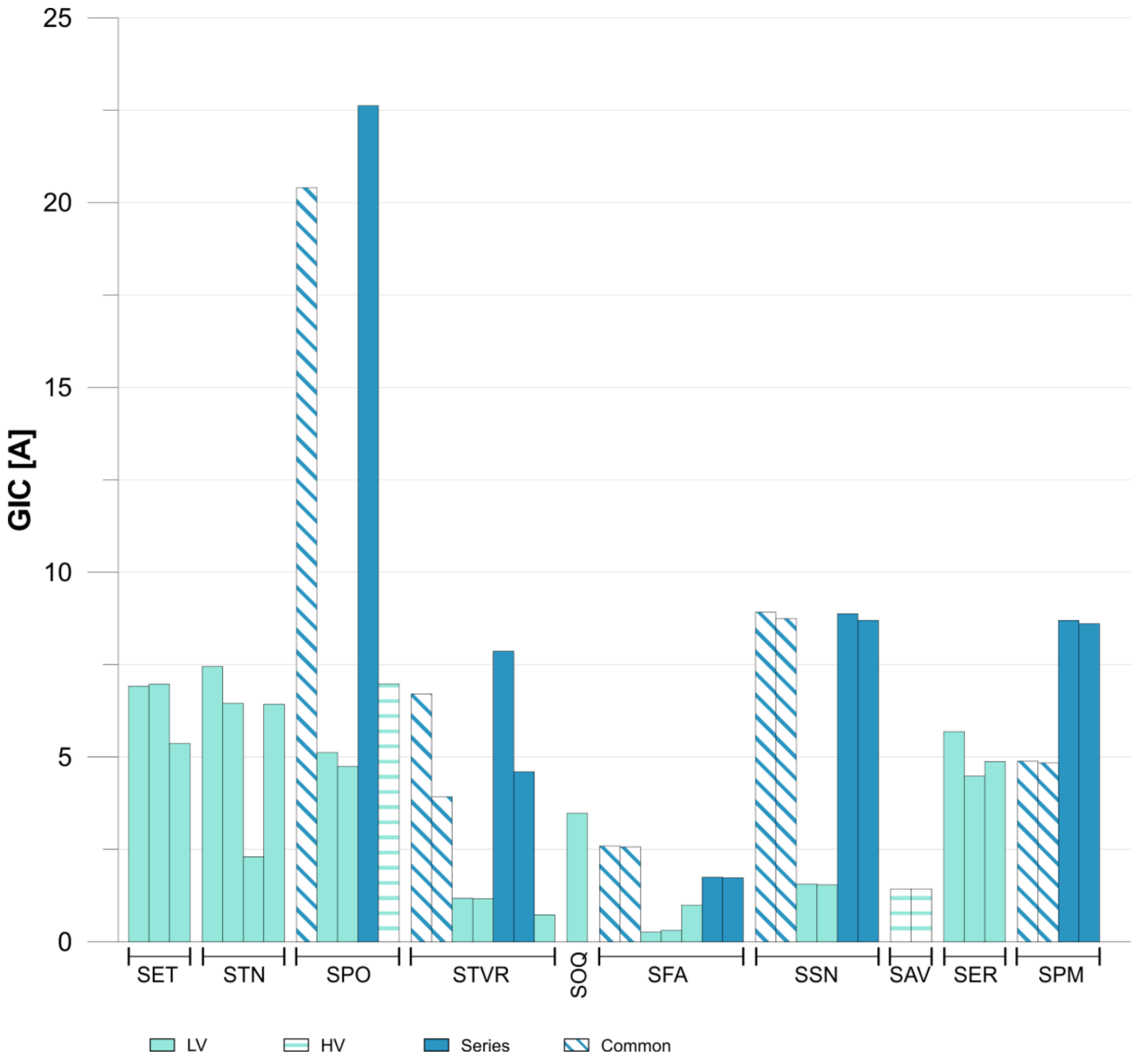

Geomagnetic Source Field

Coimbra Geomagnetic Observatory COI

- Working since 1866
- Measurements of the geomagnetic field components

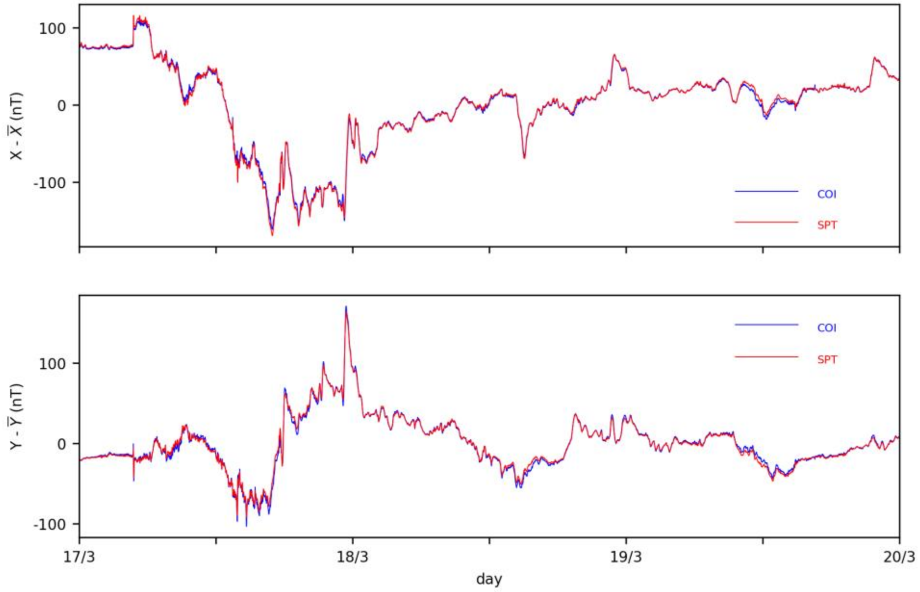

North and east components of the geomagnetic field (with the time average subtracted) during the St Patrick day storm (March 17th), both at COI (blue) and SPT – Toledo (red) observatories.

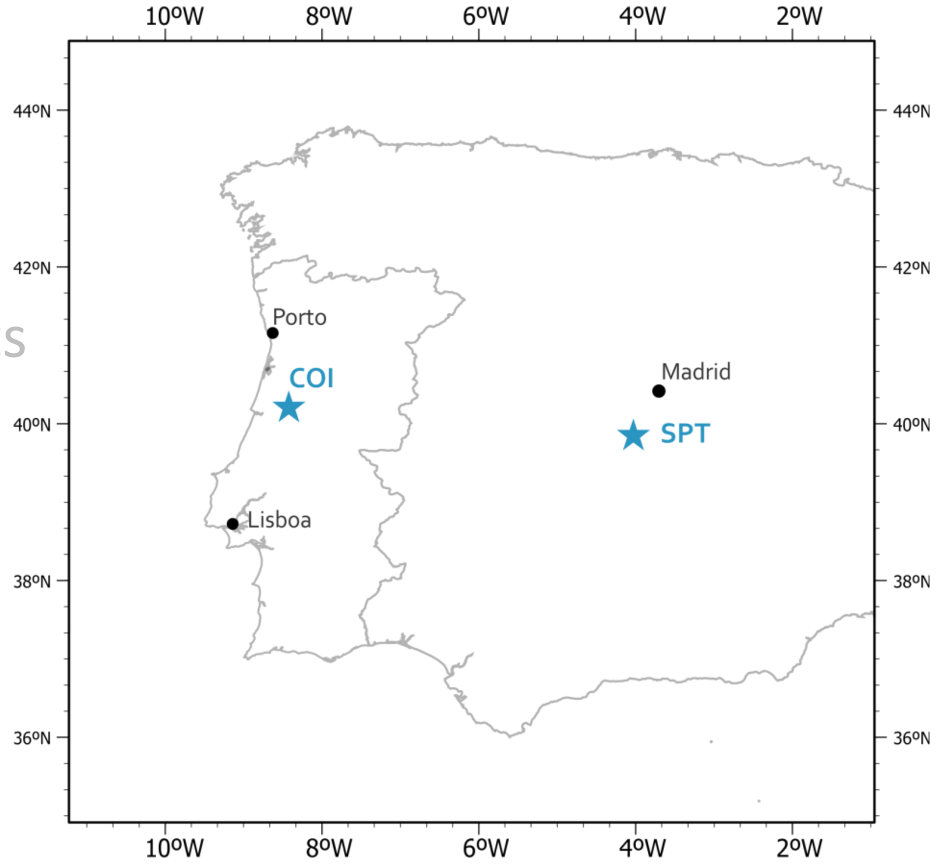

3D conductivity model

Real measurements that are planned

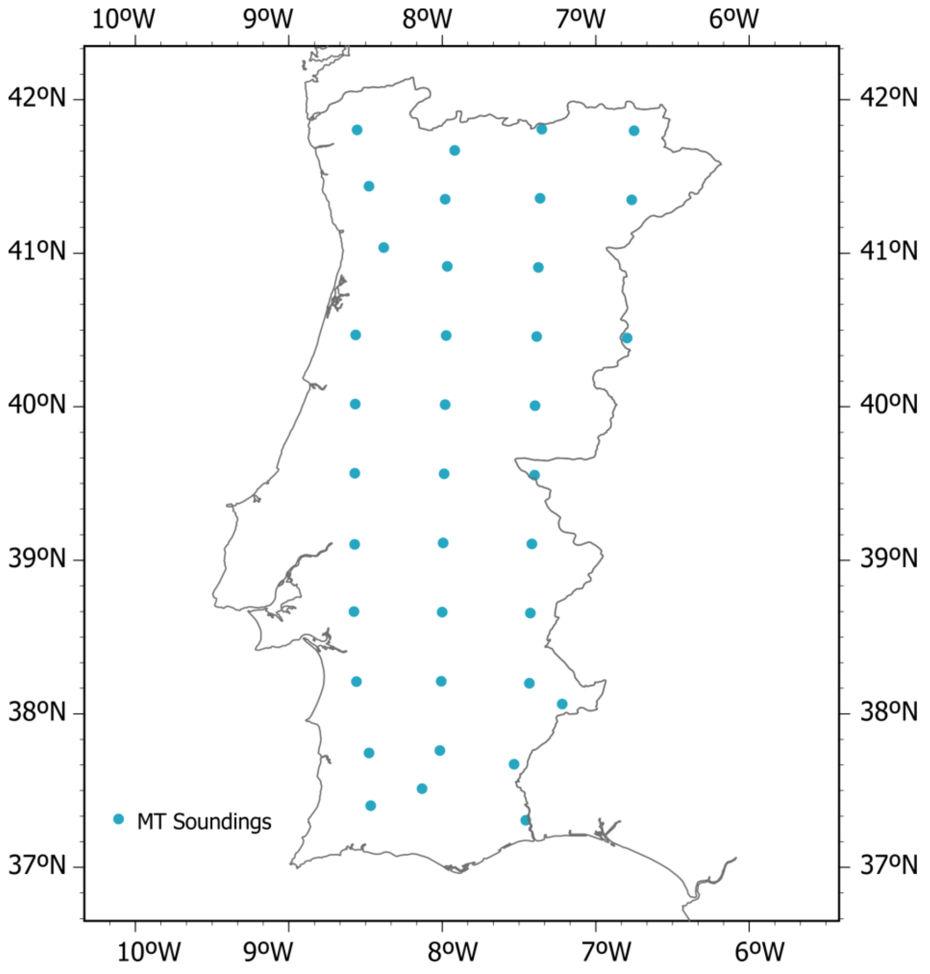

- MT Soundings ≈ 50 km

Delay due to COVID-19

Use a simplified 3D conductivity model

Simplified 3D conductivity model

Synthetic measurements

MODEM (Kelbert et al., 2014)

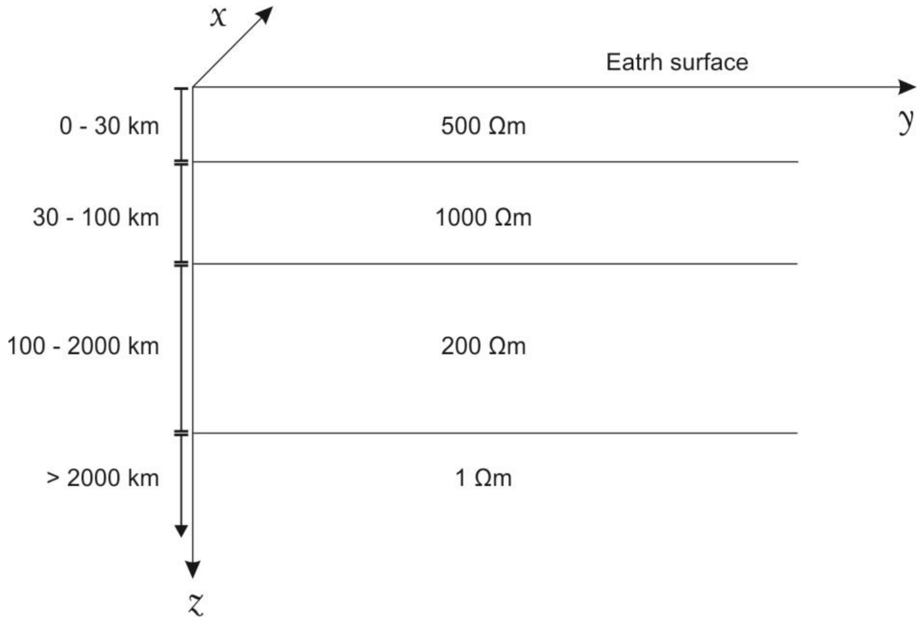

Distribution of the resistivity at mainland in depth used for the 3D simplified conductivity model, based on previous studies of the lithosphere inland (*Da Silva et al., 2007*; *Almeida et al., 2005*; *Alves Ribeiro, 2018*) and in the ocean (*Monteiro Santos et al., 2003*).

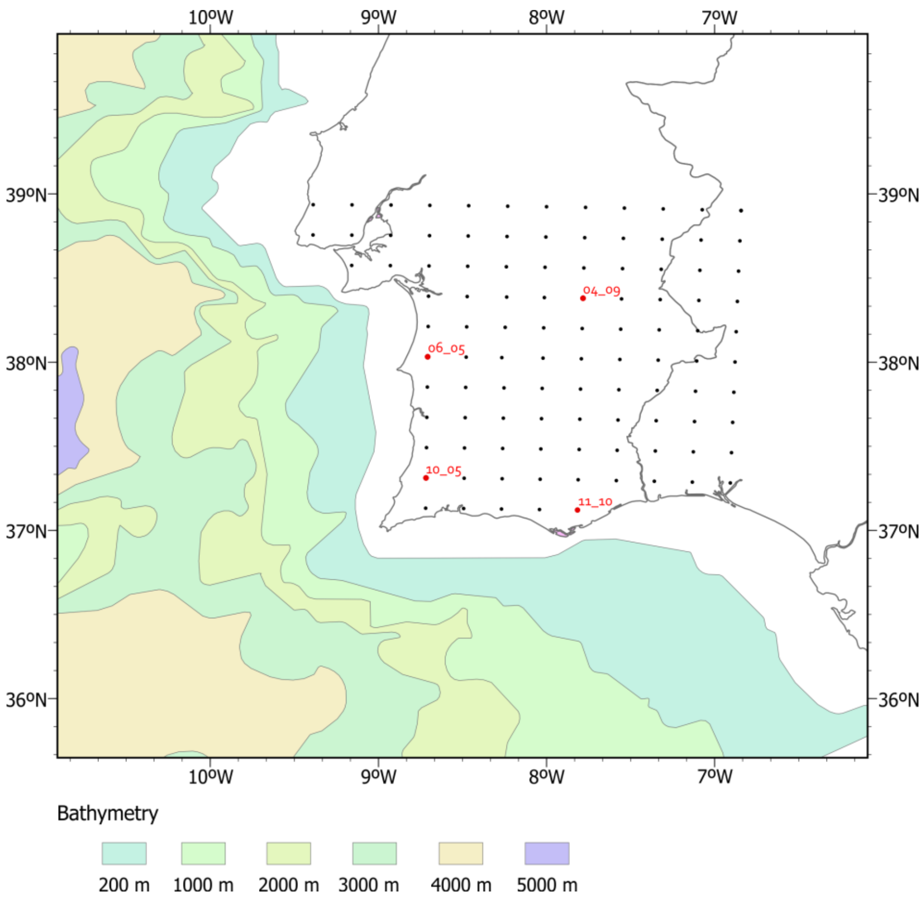

Location of the MT soundings (black and red dots) used to solve the forward modelling. Bathymetry based on ETOPO1 Global Relief Model (Amante & Eakins, 2009).

St. Patrick Storm

17.03.2015

K_p	8-
K	6
dX/dt (nT/min)	34.16
dY/dt (nT/min)	27.4

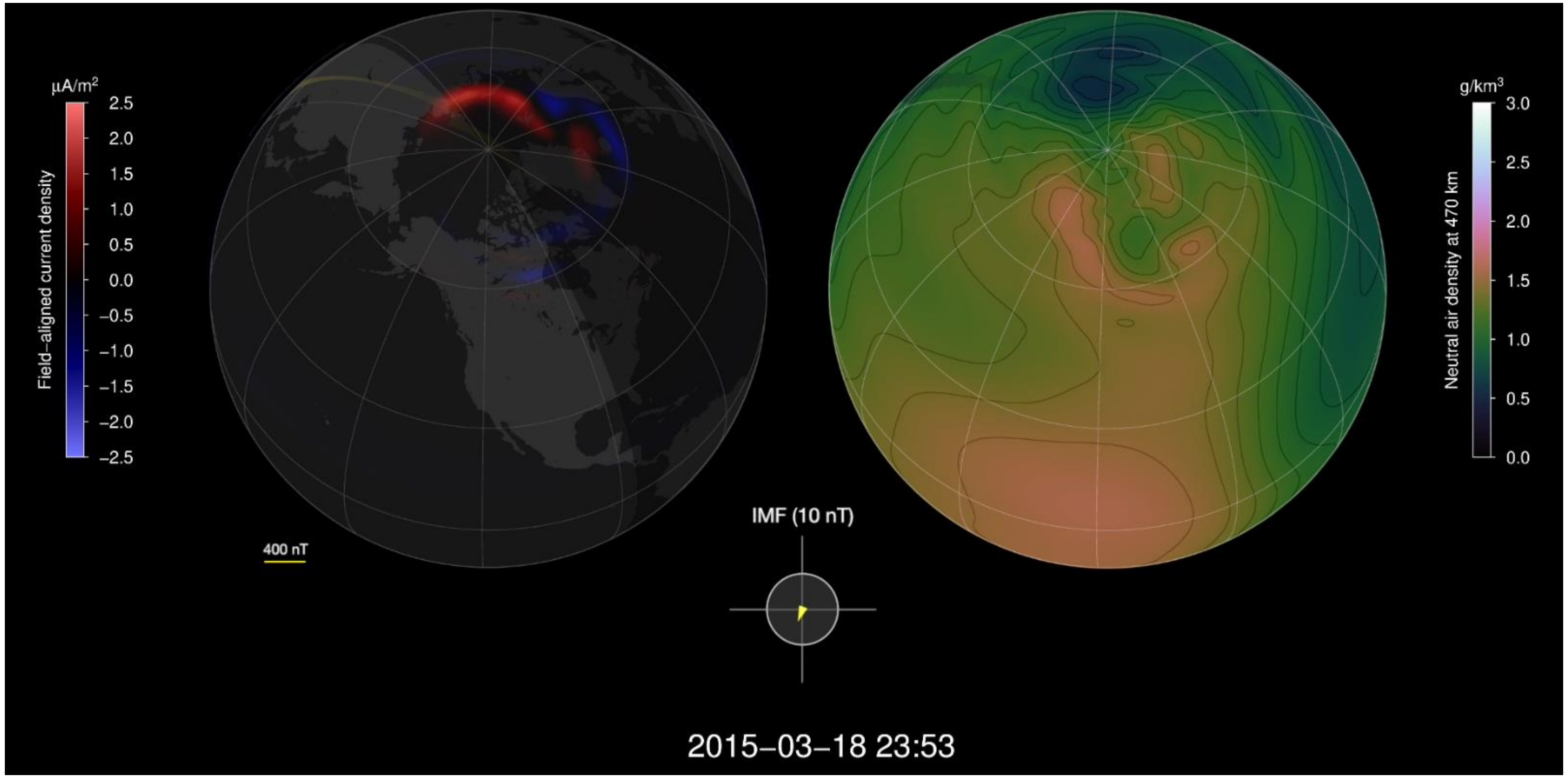

Credit: European Space Agency

St. Patrick Storm

17.03.2015

Geomagnetic field registered at COI

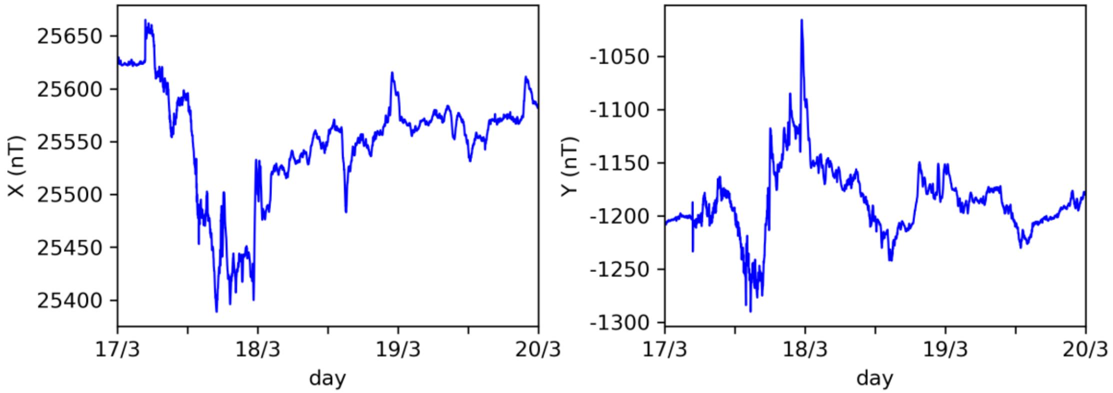

Electric field induced during the St. Patrick day storm

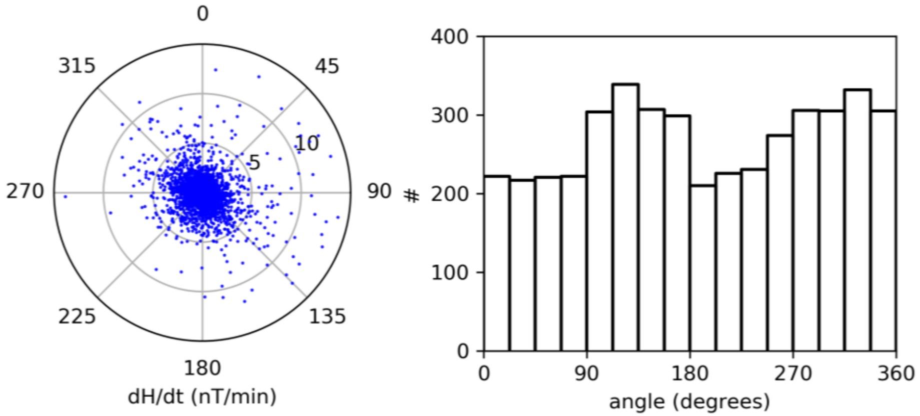

Histogram with the total number of 1-min occurrences along all possible geographical directions

St. Patrick Storm

17.03.2015

$$E_{x,y}(\omega) = \frac{1}{\mu_0}\mathbb{Z}(\omega) \times B_{x,y}(\omega)$$

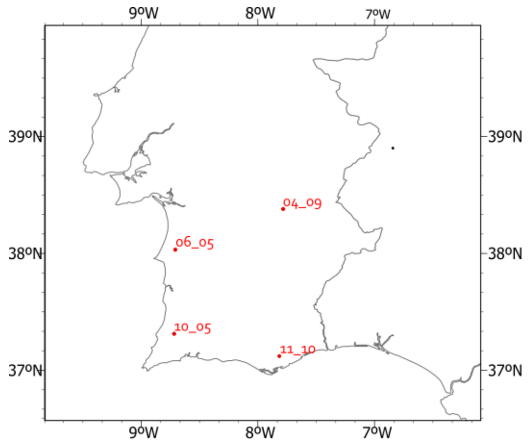

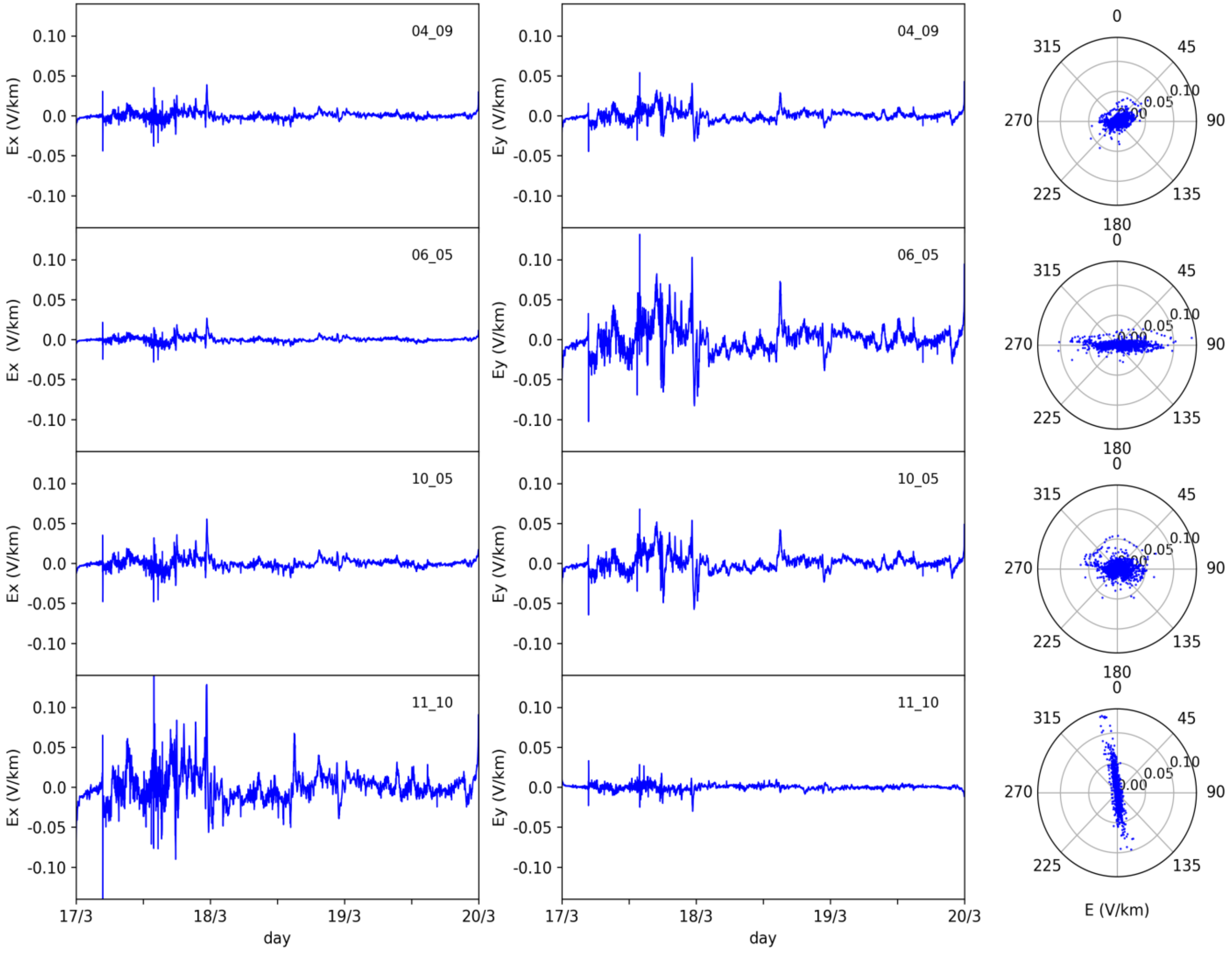

- 04_09 – E perpendicular to dH/dt

Electric field induced (left) at the four sites shown in right corner figure; polar charts for the horizontal electric field induced at the same four locations (right).

St. Patrick Storm

17.03.2015

$$E_{x,y}\,(\omega) = \frac{1}{\mu_0}\mathbb{Z}(\omega) \times \; B_{x,y}(\omega)$$

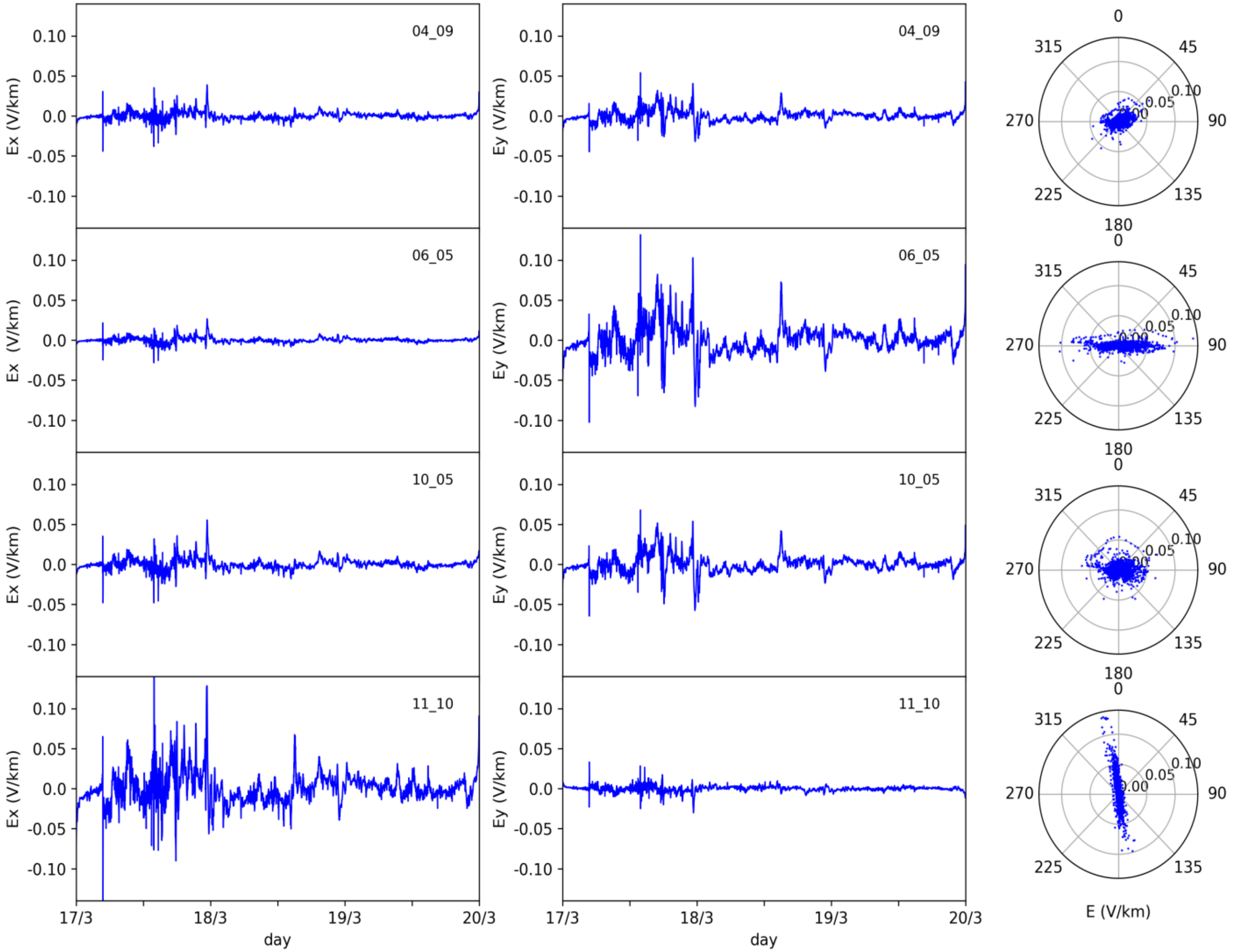

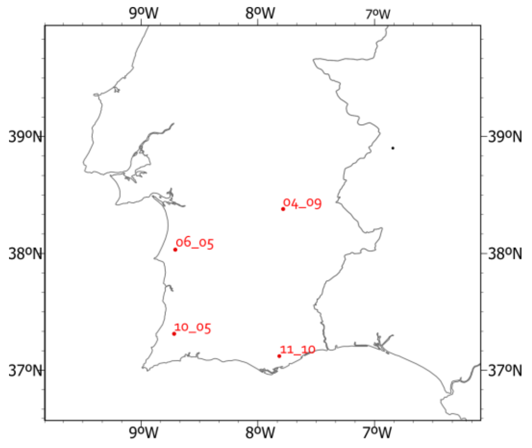

Observable ocean effect

- 06_05 – E perpendicular to the west coast
- 11_10 – E perpendicular to south coast
- 10_05 – not so visible as it suffers the effect from both west and south coast, but showing more tendency with the western coast

Electric field induced (left) at the four sites shown in right corner figure; polar charts for the horizontal electric field induced at the same four locations (right).

St. Patrick Storm

17.03.2015

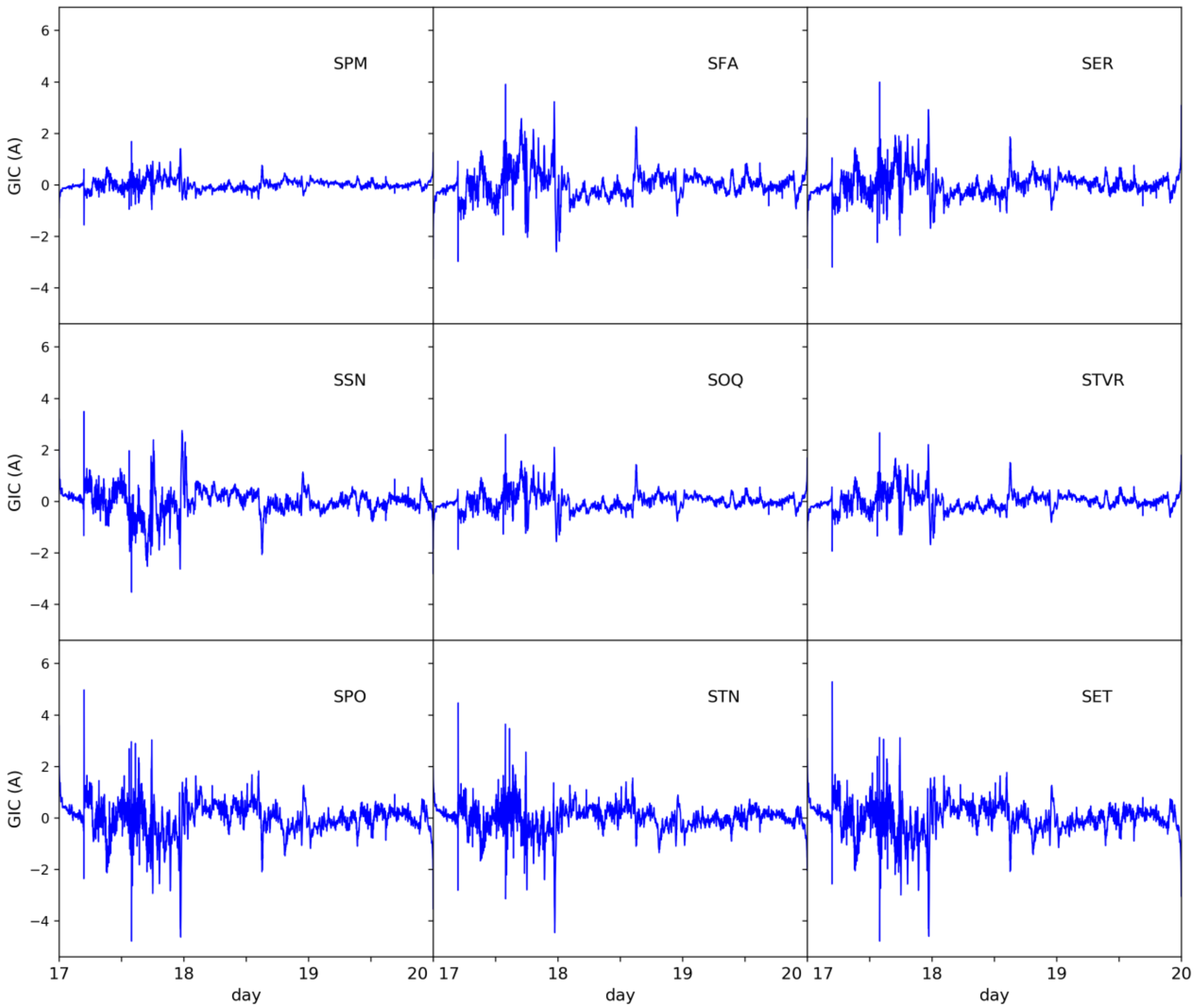

Highest GIC intensities

- Orientation of the induced E
- θ_{peak} of the substation

GIC series expected for substations in the south of Portugal

St. Patrick Storm

17.03.2015

GIC_{max} = 5.28 A

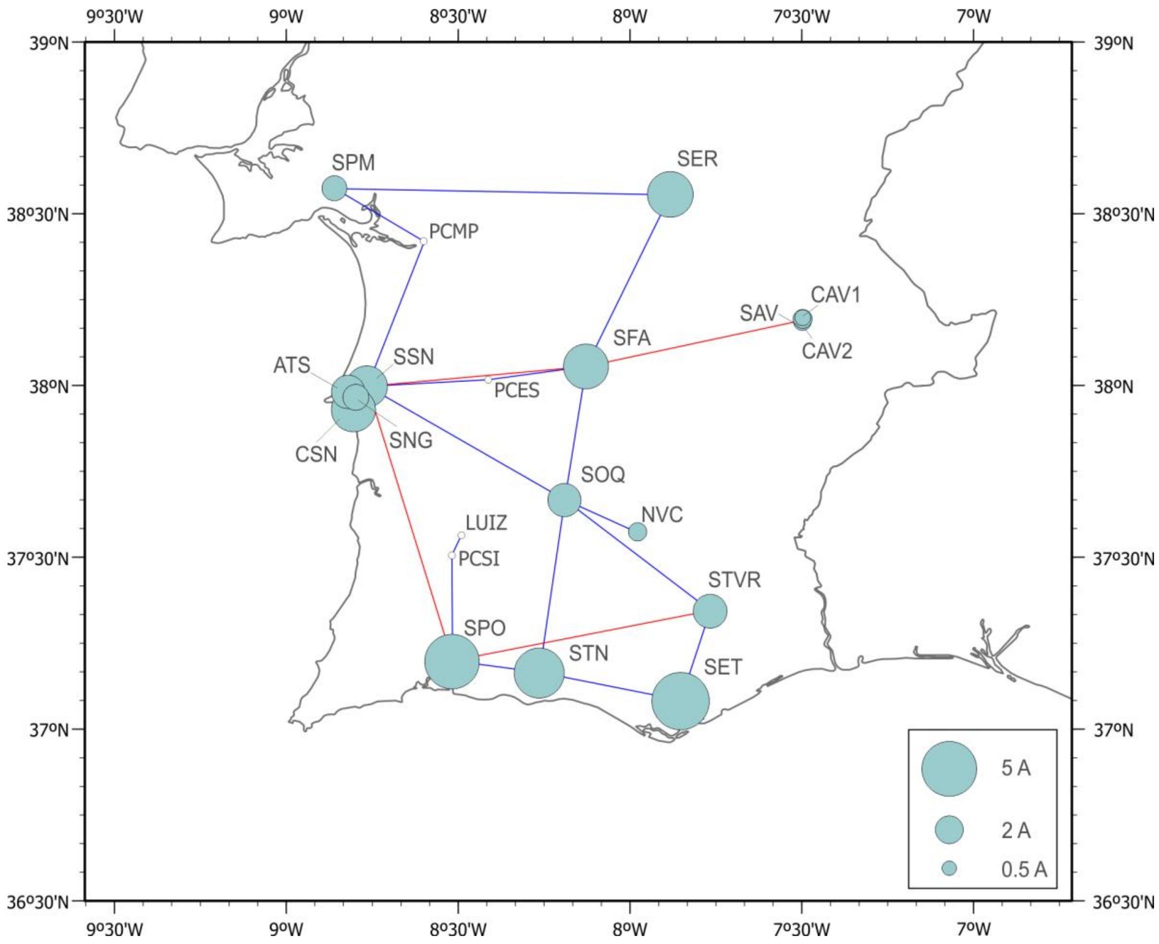

Most vulnerable

SET substation

Concluding Remarks

Uniform Electric Field – 1 V/km

- Allows us to study the vulnerability of substations with respect to the grid parameters
- SPO substation is the most vulnerable (GIC_{peak} of 110.8 A)

Good option for installing a **Hall sensor effect** in the South of Portugal

St. Patrick Storm – 17.03.15

- Highest GIC intensities depend both on the orientation of the induced E and on the θ_{peak} of the substation
- SET substation is the most vulnerable (GIC_{max} of 5.28 A)

Future Work

Network

- Extend network for all of Portugal;
- Equivalent circuit – work on collaboration with REE for creation of more precise equivalent circuit in the borders;
- Evaluate possible substation for installation of Hall sensors in the northern part of the network.

3D Conductivity model

- Resume MT data acquisition as soon as allowed;
- More precise 3D conductivity model of Portugal mainland.

GIC Sources

- Understand linear polarization of dH/dt in observed storms

References

- Almeida, Eugénio, et al. "Magnetotelluric measurements in SW Iberia: New data for the Variscan crustal structures." Geophysical research letters 32.8 (2005).
- Alves Ribeiro, J.. *Magnetotelluric studies in detecting an old suture zone and major crustal scale shear zones (Iberia)* (doctoral dissertation). Universidade de Lisboa (Portugal) (2018).
- Amante, Christopher, and Barry W. Eakins. "ETOPO1 arc-minute global relief model: procedures, data sources and analysis." (2009).
- Bailey, Rachel L., et al. "Modelling geomagnetically induced currents in midlatitude Central Europe using a thin-sheet approach." Annales Geophysicae. Vol. 35. No. 3. European Geosciences Union (2017).
- Boteler, D. H., et al. "Equivalent circuits for modelling geomagnetically induced currents from a neighbouring network." 2013 IEEE Power & Energy Society General Meeting. IEEE, (2013).
- Boteler, D. H., and R. J. Pirjola. "Comparison of methods for modelling geomagnetically induced currents." Annales Geophysicae (09927689) 32.9 (2014).
- Boteler, D. H., and R. J. Pirjola. "Modeling geomagnetically induced currents." Space Weather 15.1 (2017): 258-276.
- Da Silva, N. Vieira, et al. "3-D electromagnetic imaging of a Palaeozoic plate-tectonic boundary segment in SW Iberian Variscides (S Alentejo, Portugal)." Tectonophysics 445.1-2 (2007): 98-115.
- Kelbert, Anna, et al. "ModEM: A modular system for inversion of electromagnetic geophysical data." Computers & Geosciences 66 (2014): 40-53.

References

- Molinski, Tom S. "Why utilities respect geomagnetically induced currents." Journal of atmospheric and solar-terrestrial physics 64.16 (2002): 1765-1778.
- Monteiro Santos, Fernando A., et al. "Lithosphere conductivity structure using the CAM-1 (Lisbon-Madeira) submarine cable." Geophysical Journal International 155.2 (2003): 591-600.
- Lehtinen, M., and R. Pirjola. "Currents produced in earthed conductor networks by geomagnetically-induced electric fields." Annales geophysicae (1983). Vol. 3. No. 4. 1985.

Acknowledgement

- This study is funded by national funds through FCT (Foundation for Science and Technology, I.P.), under the project MAG-GIC: PTDC/CTA -GEO/31744/2017.

- Collaboration with REN (Rede Eletrica Nacional) was most important for the setup of the Beta network model.

- CITEUC is funded by National Funds through FCT - Foundation for Science and Technology (project: UID/MULTI/00611/2019) and FEDER – European Regional Development Fund through COMPETE 2020 – Operational Programme Competitiveness and Internationalization (project: POCI-01-0145-FEDER-006922)